Research Article | Vol. 29, No. 10 / 10 May 2021 / Optics Express 15345
Optics EXPRESS

Experimental characterization of an o-band bismuth-doped fiber amplifier

NATSUPA TAENGNOI,* KYLE R. H. BOTTRILL, YANG HONG, YU WANG, NARESH K. THIPPARAPU, JAYANTA K. SAHU, PERIKLIS PETROPOULOS, AND DAVID J. RICHARDSON

Optoelectronics Research Centre, University of Southampton, Southampton, SO17 1BJ, UK
nt1a15@soton.ac.uk

Abstract: The recent emergence of bismuth-doped fiber amplifiers (BDFAs) offers the potential to transmit high-speed WDM signals over long distances in the O-band spectral region, thereby greatly enhancing the scope of systems utilizing these wavelengths. In this paper, we present a comprehensive experimental study on several basic characteristics of an O-band BDFA based on a phosphosilicate optical fiber, including the frequency-dependent noise figure, gain tilt (static and dynamic), transient response, and polarization dependent gain. We discuss our findings and their implications on the use of BDFA technology in high bit-rate multichannel systems.

1. Introduction

The O-band spectral region, between the wavelengths of 1260 nm and 1360 nm, has been generally utilized in cost-sensitive point-to-point optical transmission links, mainly thanks to the low chromatic dispersion (CD) of standard silica single-mode fibers (the SMF-28 family) in this region and the availability of inexpensive O-band sources. O-band transmission over SMF experiences higher optical attenuation than in the C-band, mainly caused by greater Rayleigh scattering [1]. Therefore, the transmission reach in the O-band is limited to a few tens of km and effective amplification solutions are needed for this reach to be extended further.

A small variety of optical amplifiers for the O-band are already available on the market. Most notably, these include semiconductor optical amplifiers (SOAs). The amplification quality of SOAs however, is generally poorer than that of doped-fiber amplifiers, since they suffer from a relatively high noise figure (NF) and are prone to introducing signal distortions due both to the fast gain dynamics and optical nonlinearity, especially when used for the amplification of high-speed, multi-channel signals.

The development of 1.3-μm doped-fiber amplifiers has been established since the 1990s [2]. In their early implementations, fluoride glass hosts were widely used, doped with either praseodymium or neodymium [2,3]. However, several drawbacks of fluoride glasses, including their fragility, limited chemical stability and cost have limited their practicality and cost effectiveness [4]. Recently, the emergence of bismuth-doped silica fiber has introduced a promising low-noise amplification solution for wavelengths around 1.3μm that may finally prove analogous to the ubiquitous erbium-doped fiber amplifiers (EDFAs) of the C-band.

An important feature of bismuth-doped fiber amplifiers (BDFAs) is the dependency of the gain band wavelength upon the composition of their glass host (with pure silica, aluminosilicate, phosphosilicate, and germanosilicate having been experimented with) and their pump wavelength, with gain being demonstrated across wavelengths ranging from 0.6μm to 1.7μm [5–7]. For instance, a BDFA with a phosphosilicate glass-host, offering gain in the O-band between 1300 nm and 1340 nm, was first demonstrated in 2009 [8] with a max gain of 24.5 dB, using a single

#420995 https://doi.org/10.1364/OE.420995
Journal © 2021 Received 28 Jan 2021; revised 16 Mar 2021; accepted 17 Mar 2021; published 4 May 2021

Optics EXPRESS

pump and a forward pumping scheme. A BDFA that was designed to operate within the commercially used region of the O-band was presented in [9] with careful selection of the pump wavelength in a simple, single-pump BDFA enabled a maximum gain of 19 dB across a window of 1272-1310 nm and a 5.5-dB NF. Another BDFA operating within the E-band and offering a 37-nm 3-dB-bandwidth using a counter-pumping scheme at 1310 nm was presented in [10]. Moving on to the amplifier being investigated in this paper, it has been specifically designed to produce a high gain and broad bandwidth, the former being especially important in the O-band, since the propagation loss of the SMF-28 family in this band is approximately 1.5 times higher than in the C-band. The use of a bidirectional pumping scheme and a reasonably long, 150-m fiber (~1.9 times longer than that used in [9]), enabled a high gain of 26 dB, albeit with an expected increase in NF. Meanwhile, thanks to the two different pump wavelengths used in this amplifier, a 3-dB bandwidth of ~40 nm was achieved, homogeneously broadened across the gain region. Recently, the practicality of this BDFA has been demonstrated through a number of amplified transmission experiments considering either single- or multi-channel wavelength-division multiplexing (WDM) systems and a range of transmission settings [11–14].

The widespread adoption of the EDFA in C-band systems has come about not only because it exhibits gain across the lowest loss region of SMFs, but also because of its high efficiency, high gain, slow gain dynamics and low additive noise. Early in the adoption of the EDFA, its performance was extensively characterized in terms of gain, NF, nonlinear behavior, etc [1,15,16]. This parameterization provided a comprehensive understanding of the EDFA and hence allowed for its usage to the fullest extent, in systems ranging from single-channel links to modern, high-speed WDM transmission. On the other hand, the BDFA, which is a newly developed O-band amplifier, still requires such characterization to support its future use in O-band transmission.

In this paper, we present an experimental characterization of a fully-boxed, in-house built O-band BDFA. Our characterization covers four different performance metrics of the amplifier, namely the frequency-dependent NF, the gain tilt (both static and dynamic), the transient response, and the polarization dependent gain (PDG). By performing a frequency resolved measurement of the NF in the electrical domain, we demonstrate that this amplifier exhibits a NF of ~6.3 dB over its flattest gain region (1330-1360 nm) with little (undetectable in our experiment) excess low-frequency noise. With regards to the gain characterization, we demonstrate that this BDFA possesses near-zero gain slope between the wavelengths of 1330 nm and 1360 nm, a critical factor for WDM transmission. The dynamic-gain tilt is measured to be less than 0.3 dB/nm and the transient response rapidly falls to below 1 dB at frequencies greater than 60kHz. This feature is important when operating in WDM systems with dynamically added/dropped channels. In addition, the PDG value of this BDFA is well below 0.64 dB for all tested wavelengths. Note that this paper extends upon the preliminary results presented in [17] with additional characterizations and discussion. Although these BDFA characterization measurements have been carried out in a particular amplifier (our in-house built BDFA, as used in the transmission experiments reported in [12–14]), we consider that this early report is indicative of what is possible in Bismuth doped fibers and we can reasonably expect the performance only to improve over time with further optimization.

2. Bismuth-doped phosphosilicate fiber amplifier

The amplifier tested in this paper was an in-house built O-band BDFA [18], with the configuration shown in Fig. 1. The amplifier contained a 150-m length of bismuth-doped phosphosilicate fiber (BDF). The BDF was bidirectionally pumped at two wavelengths (1240nm and 1267nm) to broaden and flatten the gain spectra. The total pump power was 720mW. WDM multiplexers/de-multiplexers were placed at each end of the gain medium to couple/decouple the signal.

Optics EXPRESS

Optical isolators (ISOs) were used to control the propagation direction and prevent any back-propagation/reflection in the amplifier. The gain provided by the BDFA was around 23-26dB between 1325nm and 1365nm. Recently, it has been demonstrated that the gain bandwidth of this O-band BDFA can be broadened to cover substantial parts of both the O- and E- band regions, as reported in [19].

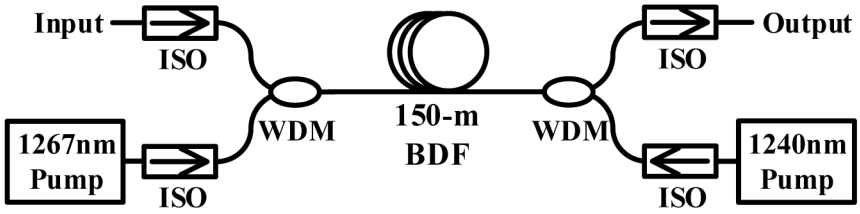

Fig. 1. The configuration of the in-house built BDFA.

3. Characterization: set-ups and results

This section details the characterization set-ups used and the results obtained. It is divided into four parts to report the measurements of frequency-dependent NF, gain tilt, transient response, and PDG.

3.1. Frequency-dependent noise figure

The noise performance of an optical amplifier is typically quantified by the NF. One factor which determines the noise characteristics of an amplifier is the fiber length. The length of our BDFA is much longer relative to that of a typical EDFA (which has a length of tens of meters). An experimental study of the gain performance of the BDFA provided in [20] showed that by increasing the bismuth concentration and reducing the diameter by 20%, the fiber length could be reduced to 98 m, although the outcome was to achieve a lower gain. This could be due to gain quenching effects at high dopant concentration [21], unsaturable loss, and the amount of OH absorption [20]. Additionally, the long fiber span directly affects the pump absorption which will be gradually bleached over the length of the fiber [22]. In general, the NF is not constant in frequency. One major reason for this is because multi-path interference, created by effects, such as Rayleigh scattering (RS), produces interferometric/internal noise [21,23]. The necessarily long fiber length implies a risk of elevated low-frequency NF and elevated frequency-flat NF due to the intrinsic loss (per unit length) of the fiber [22]. To quantify the frequency-dependent NF, we adopted an electrical measurement technique based on source-noise subtraction (see [15] for more details). For added context, we compared the performance of the BDFA to that of a commercial O-band SOA (Thorlabs-BOA1036S).

The experimental setup of the electrical NF measurement is shown in Fig. 2(a). The transmitter (Tx) consisted of a single, shot-noise limited continuous-wave (CW) tunable laser (LAS), which was launched into the amplifier with adjustable input power (P_{in}), controlled through an attenuator (ATT-1). At the amplifier output, an optical bandpass filter (OBPF, 1.2-nm bandwidth) followed by a second attenuator (ATT-2) were used to control the detected optical bandwidth and the received power (P_{rx}), respectively. This arrangement filtered out the spontaneous-spontaneous beat noise and ensured that signal-spontaneous beat noise dominated the system [15]. The wavelength range over which our measurements were conducted was determined by the tunability range of the laser used (from 1260 nm to 1360 nm). At the receiver (Rx), the signal was detected using a photodetector (PD) and was then fed to a radio frequency (RF) spectrum analyzer (RFSA).

The electrical NF can be calculated from the excess noise produced by the BDFA when amplifying a CW probe signal with a given input power (P_{in}). The NF was calculated using

Optics EXPRESS

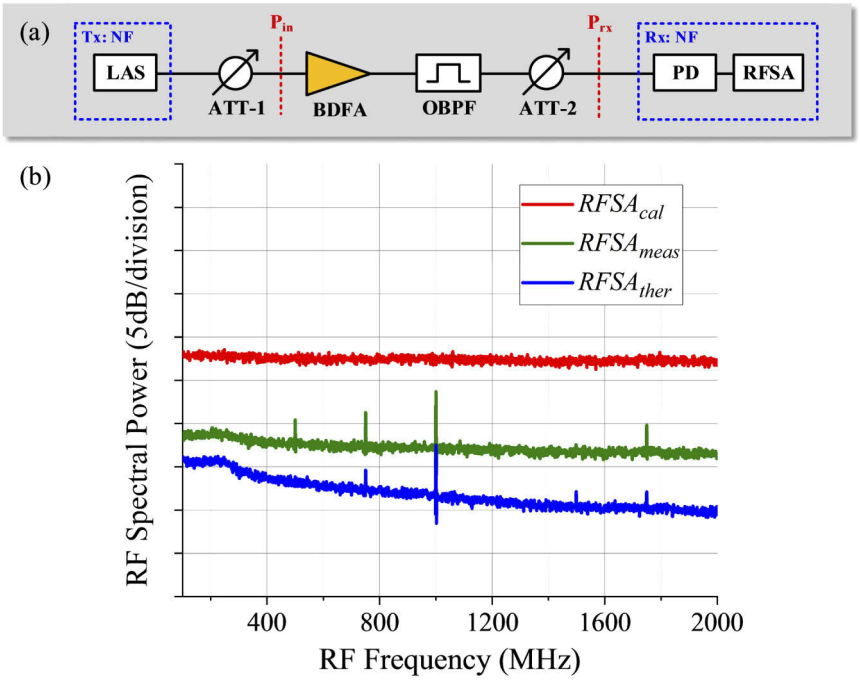

Fig. 2. (a) Experimental setup for electrical NF measurement and (b) an example of electrical power spectra measured by the RFSA that were used to determine the electrical NF of the BDFA at the wavelength of 1350 nm and the input power (P_{in}) = -20dBm.

Eq. (1), derived in [15]:

$$NF = 10log\left(\frac{1}{2h\nu G^2 P_{in}}\left(\frac{RFSA_{meas}(f) - RFSA_{ther}(f)}{RFSA_{cal}(f)/k_{RIN}(f)} - PD_{shot\ noise}\right) + \frac{1}{G}\right) \quad (1)$$

where, h is the Planck's constant, ν is the measured signal frequency, G is the optical gain. The RF spectra to be measured are as follows: $RFSA_{meas}(f)$ is the RF spectrum of the amplified signal (measured by the RFSA), $RFSA_{ther}(f)$ is the RF spectrum of the thermal noise of the receiver, $RFSA_{cal}(f)$ is the RF spectrum of a calibration source with a known frequency dependent relative intensity noise (RIN), given by $k_{RIN}(f)$. Finally, $PD_{shot\ noise}$ is the shot noise from photo-detection (calculated and not measured as it sat below the thermal noise).

As seen from the equation above, the calculation of the NF is an involved process [15], the full explanation of which is beyond the scope of this work. However, for illustrative purposes, plots of $RFSA_{meas}(f)$ (green line), $RFSA_{ther}(f)$ (blue line), and $RFSA_{cal}(f)$ (red line) are provided in Fig. 2(b), for a wavelength of 1350 nm and input power of -20dBm. Equation (1) also shows that it is necessary to obtain the receiver calibration, $k_{RIN}(f)$ (which can be achieved using a variety of methods discussed in [15], here we use the 'RIN transfer' method), and consider the shot noise term, $PD_{shot\ noise}$ (measured through the current drawn by the PD and its responsivity).

The frequency-dependent NF results for the BDFA at an input power of -20dBm at various wavelengths are shown in Fig. 3(a). Note that this input power was chosen to avoid operating the amplifier in saturation. We observe that the BDFA's NF exhibits a flat frequency response across the frequency range from 100 MHz up to 2000MHz, i.e. it has no pronounced low-frequency noise components [15]. Figure 3(b) shows the averaged NF between 100 MHz and 2000MHz as it varies with wavelength. The minimum NF is observed to be ~6.3 dB at 1340 nm and increases towards both edges of the plot, reflecting the shape of the gain profile (red dashed line

Optics EXPRESS

in Fig. 3(b)). The effect of the NF reduction in the regions of increased gain is consistent with the optically measured (and hence not frequency resolved) NF results reported in [18] for the very same amplifier. In addition, the characterization of the input power dependency of the averaged NF is shown in Fig. 4 for a wavelength of 1350 nm. The NF increases with increasing input power, a behavior typical of all optical amplifiers, originating from the gain compression due to the onset of saturation [16].

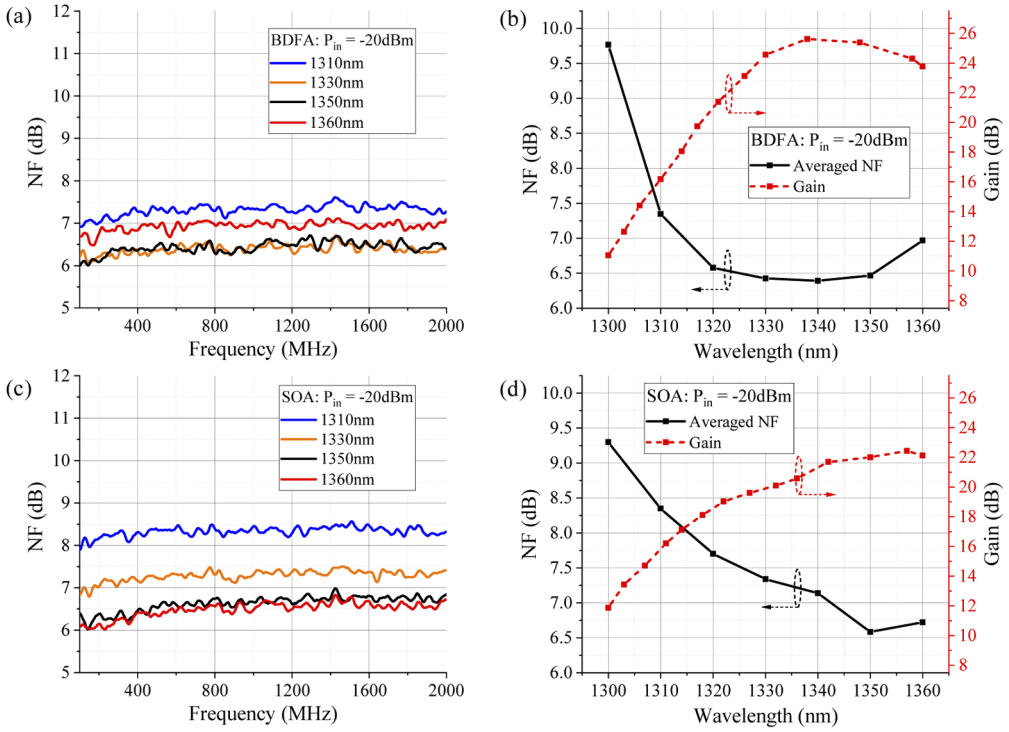

Fig. 3. (a) frequency dependent NF of the BDFA, (b) averaged NF of the BDFA as it varies with wavelength, (c) frequency dependent NF of the SOA, and (d) averaged NF of the SOA as it varies with wavelength.

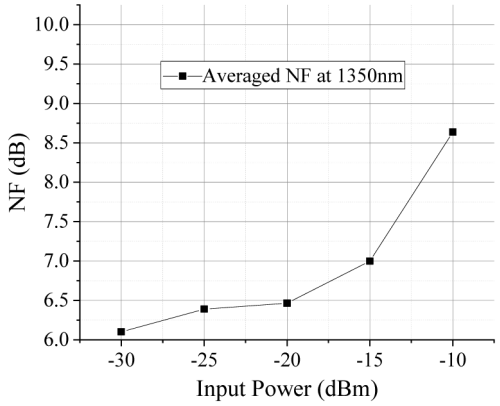

Fig. 4. Averaged NF of the BDFA at the wavelength of 1350 nm as it varies with input power.

Optics EXPRESS

A similar NF measurement carried out on an O-band SOA is reported in Fig. 3(c) and Fig. 3(d), which show the frequency-dependent and averaged NF, respectively. The results obtained on the SOA confirm the superior performance of the BDFA (over the tested region), since they show both a lower gain and a higher NF, which are a consequence of the coupling loss, the cavity structure, and population inversion related effects [24].

3.2. Gain tilt

The gain provided by an optical amplifier is a function of the optical wavelength. The gain tilt refers to the gradient of the variation of gain with wavelength. A low gain tilt is essential to the in-line amplification of multi-channel WDM communication signals in order to prevent the various channels from experiencing unequal gain, which will result in performance variations across the gain spectrum. The gain tilt may be further accentuated by either adding or dropping channels, and several methods have been proposed to control/reduce its effects, such as using an out-of-band signal of controllable power [25] and using gain flattening filters (GFFs) [26].

There are two types of gain tilt typically defined: *static* and *dynamic*. The static gain tilt m_{st} is just the derivative of the amplifier's gain spectrum, see Eq. (2):

$$m_{st}(\lambda_0, P_{in}) = \frac{G_{st}(\lambda_0 + \Delta\lambda, P_{in}) - G_{st}(\lambda_0 - \Delta\lambda, P_{in})}{2\Delta\lambda} \tag{2}$$

where, $G_{st}(\lambda_0 \pm \Delta\lambda, P_{in})$ is the signal gain measured at a wavelength of $\lambda_0 \pm \Delta\lambda$ as a function of its input power (P_{in}). The static gain tilt is therefore related to the gain flatness of the amplifier and in practice, is measured using a single input beam.

Conversely, the study of dynamic gain tilt requires a two-wave system. The gain experienced by a small (probe) signal is monitored in the presence of a large signal in its vicinity, the purpose of which is to saturate the amplifier. The dynamic gain tilt can imply a change in the amplifier inversion state caused by the amplifier's saturation when sweeping the large signal. This is because, when the amplifier begins to saturate, its ability to maintain the equilibrium state decreases. This eventually leads to cross-gain saturation, resulting in gain fluctuations on the small signal. The dynamic gain tilt (m_{dy}) is calculated from Eq. (3):

$$m_{dy}(\lambda_0, P_h) = \frac{G_{sm}(\lambda_0 + \Delta\lambda, P_h) - G_{sm}(\lambda_0 - \Delta\lambda, P_h)}{2\Delta\lambda} \tag{3}$$

where $G_{sm}(\lambda_0 \pm \Delta\lambda, P_h)$ is the small-signal gain measured at a wavelength $\lambda_0 \pm \Delta\lambda$ with a holding power (P_h) of the large signal, and $\Delta\lambda$ is the measuring range.

The experimental setup used for the gain tilt measurement is shown in Fig. 5(a). We used two wavelength-tunable CW lasers (LAS-1 and LAS-2) coupled together with a 3-dB coupler at the transmitter, followed by the same configuration of attenuators, amplifier and tunable filter as in the previous section, and analyzed the received signal through an optical spectrum analyzer (OSA). Both lasers were tunable in the 1300-nm–1360-nm region. LAS-2 was switched off in the static gain tilt measurement, and the measurement was repeated for various input powers (P_{in}) of LAS-1. Both lasers were switched on in the dynamic gain tilt measurement. The wavelength spacing between the two lasers ($\Delta\lambda$) was kept constant at 2nm, and their power difference was set to 30dB. Note that the spacing was selected appropriately to spectrally resolve the probe and the saturating signal using the OSA (which was operated with a resolution of 0.1nm). The power of the large signal (P_h) was varied (while maintaining a 30-dB power difference between the two signals) to observe the saturation behavior of the amplifier. Consequently, the total output power of the amplifier was effectively governed only by the saturating signal.

The gain tilt results are shown in Fig. 5(b). As before, the tested wavelengths were limited by the tunability range of the CW laser. The static gain tilts at various input powers (−5, 0, 5, and 10dBm) into the BDFA are plotted in the blue lines. The static gain tilt decreases with increasing

Optics EXPRESS

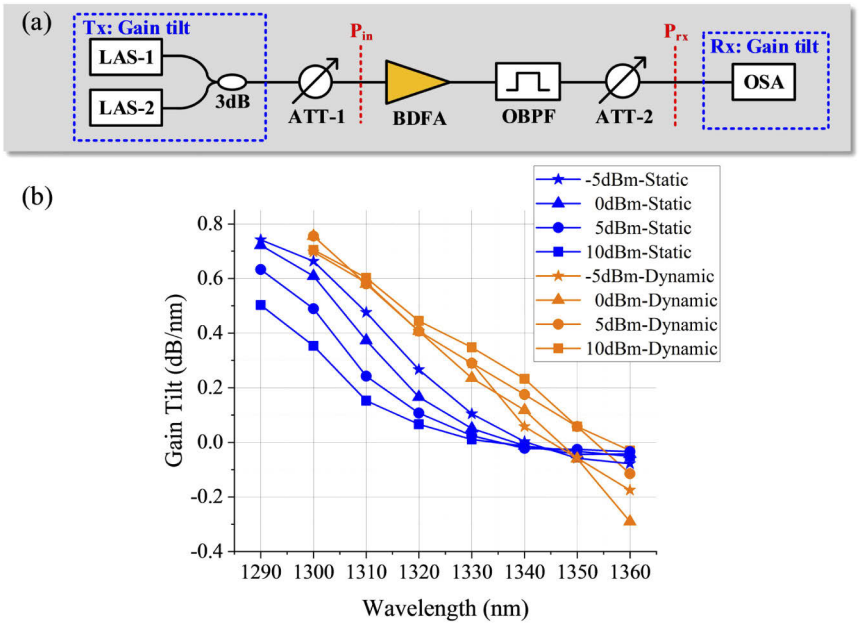

Fig. 5. (a) Experimental setup for gain tilt measurement and (b) gain tilt results.

wavelength. The higher the input power, the broader the flat region of the static gain tilt. This means that increasing the input power can flatten the amplifier's gain spectrum, as is typical. All lines cross the 0dB/nm point at a wavelength of 1340nm, which is where the peak gain of the amplifier occurs. At even longer wavelengths, the static gain tilt becomes slightly negative (but still close to zero) as the measurement traces out the decreasing gain at the upper wavelength edge of the gain spectrum. The cluster of the static gain tilt plots around the zero line also indicates the gain flatness of the amplifier at the wavelength range 1340-1360nm. This characteristic is especially important for multi-span links where reach can be limited by an uneven band spectrum at the receiver due to accumulated gain tilt from successive amplification stages.

The results of the dynamic gain tilt measurement are plotted in orange in Fig. 5(b). Note that the points for the dynamic gain are subject to more measurement noise than for the static gain because the signal power measured in the former case is 30 dB lower than the latter case. The plots of different P_h show similar behavior in the range 1300-1320 nm. However, they begin to spread out from one another in the region of peak gain (from 1330 nm onwards). As the amplifier provides a maximum gain in this wavelength region, it becomes more sensitive to saturation at higher input power levels (high holding power), leading to more prominent cross-gain saturation. However, the amount of dynamic gain tilt arising in the BDFA (across the range where the gain is flattest, 1330-1360nm) is relatively low (<0.4dB/nm), which implies that the amplifier can tolerate rapid changes in the input power, caused e.g. by adding or dropping WDM channels.

3.3. *Transient response*

Since signals copropagating in an optical amplifier can share the same source of gain (excited ions), a sudden change in the power of one signal can lead to a transient change in the gain of another, leading to a transient gain response, which may compromise the performance of the amplified signals. The response time of the process of cross-gain modulation depends on the carrier lifetime of the amplifier: the shorter the carrier lifetime, the faster the response. Doped-fiber amplifiers, in general, have a long lifetime relative to other amplifiers, such as SOAs

Optics EXPRESS

[20,24]. Therefore, the gain of a doped-fiber amplifier varies slowly with input power. This, in turn, implies that only low-frequency variations in signal input power affect the amplifier gain and hence the signal gain only varies with the "average" signal input power.

Typically, the transient response can be measured from saturation-induced crosstalk on a small probe signal in a two-channel system. Note that the saturation-induced crosstalk is unaffected by the channel spacing since it is a result of decreasing carrier density [27]. We measured the transient response by determining the power excursion of the probe signal. The setup used in this measurement is shown in Fig. 6(a). As before, we used two laser sources at the transmitter. One channel at λ=1343nm was unmodulated and was used as a small probe signal. The other channel at λ=1360nm was modulated by a Mach-Zehnder modulator (MZM) with a square wave and was used as a saturating input signal with $P_{in,sat}$=5dBm. The power ratio between the two signals was 30dB. After combining the two channels with a 3-dB coupler, they were launched into the amplifier, filtered by an OBPF to receive only the probe signal at the photodetector, and analyzed on an oscilloscope (OSC).

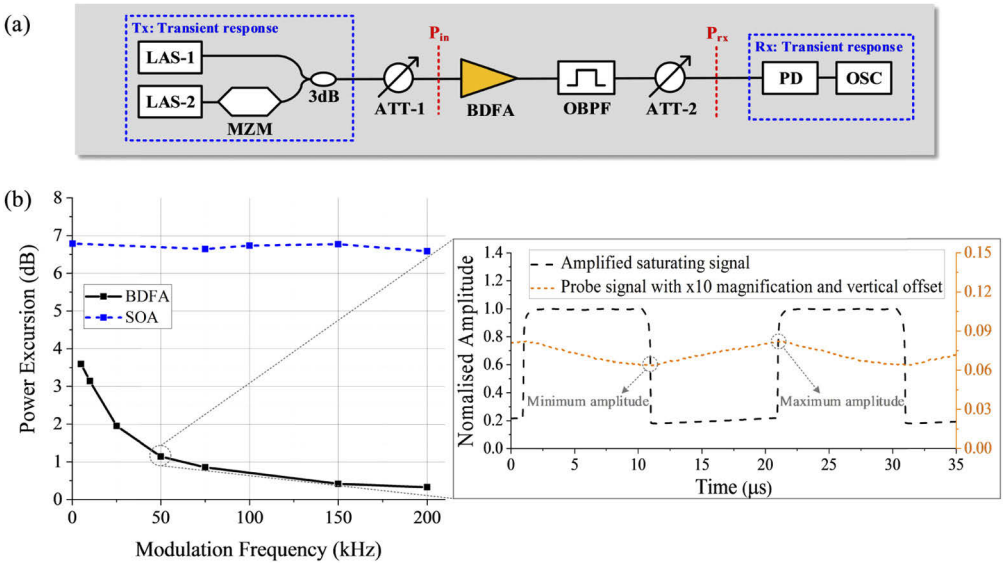

Fig. 6. (a) Experimental setup for transient response measurement and (b) power excursion of the small probe signal as a function of the modulation frequency (inset shows the optical signals modulated at 50kHz, as observed on the OSC).

An example of the optical signals modulated at 50kHz as observed at the OSC after amplification in the BDFA is shown as an inset in Fig. 6(b). The black line is the amplified saturating signal, while the orange line is the probe signal. The power excursion, measured on the probe signal (the ratio of the maximum amplitude to the minimum amplitude of the oscilloscope trace) [15], is caused by the saturation-induced crosstalk. In addition, we also measured the transient response of our O-band SOA. The BDFA's and SOA's transient response results are plotted in Fig. 6(b) in terms of power excursion as a function of the modulation frequency. The results show that, in stark contrast with the SOA, the BDFA's transient response noticeably drops with increasing modulation frequency, which is in accordance with the long carrier lifetime (slow response) in doped-fiber amplifiers. Note that the carrier lifetime of the amplifier depends on the chemical composition of the gain medium (for instance, the dopant concentration and the host glass). The lifetime of the BDF in this amplifier is around 600μs, as reported in [20].

Optics EXPRESS

3.4. Polarization dependent gain

In general, optical amplifiers provide a different amount of gain on each polarization, giving rise to the so-called polarization dependent gain (PDG). Unlike SOAs, which typically require the adoption of a polarization diversity scheme in order to amplify signals of random polarization [28], doped fiber amplifiers typically have low PDG [29] and are therefore more attractive.

The setup for the PDG measurement of the BDFA is shown in Fig. 7(a). At the transmitter, one CW laser was followed by a polarization scrambler (PolScr), 100Hz rate, to traverse all polarization states to search for the maximum and minimum power of the amplified signal which was observed using a power meter (POW). The PDG was given by the difference between the maximum and minimum powers measured. Note that we did not perform a comparison with the O-band SOA in this case, since this was a single-axis device with a polarization extinction ratio of around 18 dB. The polarization dependent loss (PDL) of the measurement set-up was found to be less than 0.07dB.

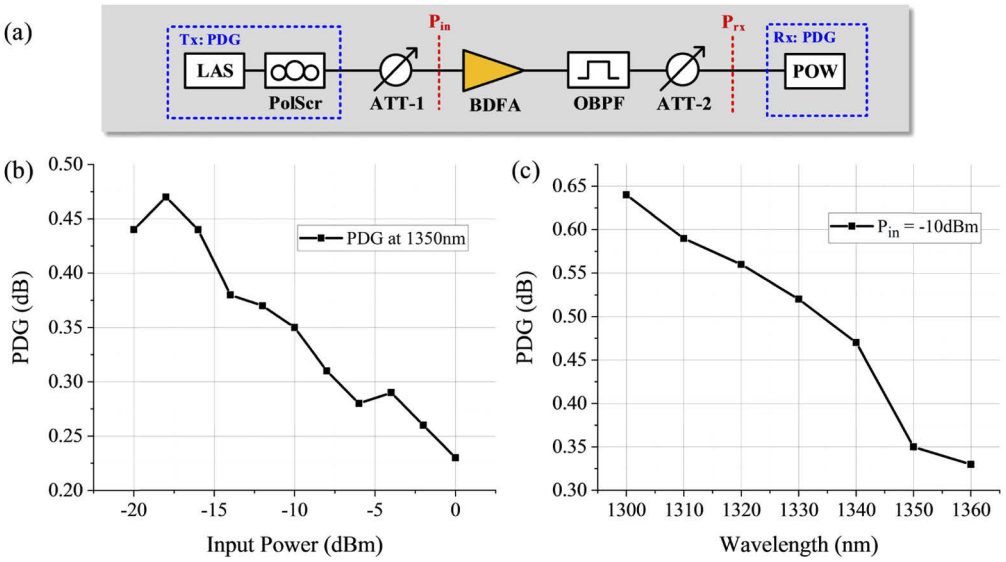

Fig. 7. (a) Experimental setup for PDG measurement, (b) and (c) PDG results of the BDFA at 1350 nm with varied input power and wavelength dependent PDG at -10-dBm input power, respectively. Note that the input power was measured at the input of the amplifier, at the point P_{in} in (a).

The PDG results at a wavelength of 1350nm as a function of the input power into the BDFA are presented in Fig. 7(b). The PDG tends to decrease with an increase in input power. This is largely because the amplifier approaches saturation as power increases. We also observe that the PDG of this BDFA decreases with increasing wavelength (see Fig. 7(c)). This could be due to a polarization mode dispersion (PMD) induced "scrambling" of the relative polarization states of the pumps and signal, which increases with increasing pump-signal wavelength separation [30]. The PDG from the plot is at all points less than 0.64dB.

4. Conclusion

This work contributes to the developing, comprehensive characterization of phosphosilicate O-band BDFAs. We presented a set of experimental measurements covering electrical NF, gain tilt, transient response, and PDG. These first measurements of this type in a BDFA show that the amplifier has no excessive low-frequency noise with a typical NF of 6.3 dB around the flat

Optics EXPRESS

peak region of the gain profile. Regarding the gain characterization, we demonstrated that the BDFA produced a near-zero gain slope from 1330 nm to 1360 nm wavelengths. The value of the dynamic-gain tilt was <0.3 dB/nm and the transient response rapidly dropped to <1 dB at modulation frequencies beyond 60kHz. A comparison has shown that the BDFA has a much slower response than a typical O-band SOA. This property is particularly important when adding or dropping channels in WDM networks. In addition, our measured PDG value of this BDFA was <0.64 dB across the tested wavelengths, which is in line with conventional doped-fiber amplifiers.

Altogether, not only do these measurements confirm the suitability of the BDFA for use in modern WDM systems but they also form part of an ongoing parameterization of BDFAs which will be essential for their deployment in systems applications.

Funding. Engineering and Physical Sciences Research Council (EP/P030181/1, EP/S002871/1).

Disclosures. The authors declare no conflicts of interest.

Data availability. The data for this work is accessible through the University of Southampton Institutional Research Repository DOI: 10.5258/SOTON/D1780.

References

1. G. Agrawal, *Fiber-Optic Communications Systems* (Wiley, 2011).
2. M. Brierley, S. Carter, P. France, and J. E. Pederson, "Amplification in the 1300 nm telecommunications window in an Nd-doped fluoride fibre," Electron. Lett. **26**(5), 329–330 (1990).
3. J. S. Wang, E. M. Vogel, E. Snitzer, J. L. Jackel, V. L. da Silva, and Y. Silberberg, "1.3 μm emission of neodymium and praseodymium in tellurite-based glasses," J. Non-Cryst. Solids **178**, 109–113 (1994).
4. W. J. Miniscalco, L. J. Andrews, A. Thompson, L. J. Quimby, L. B. Vacha, and M. G. Drexhage, "1.3 μm fluoride fiber laser," Electron. Lett. **24**(1), 28–29 (1988).
5. E. Dianov, "Bismuth-doped optical fibers: a challenging active medium for near-IR lasers and optical amplifiers," Light: Sci. Appl. **1**(5), e12 (2012).
6. I. A. Bufetov, S. L. Semenov, V. V. Vel'miskin, S. V. Firstov, G. A. Bufetova, and E. M. Dianov, "Optical properties of active bismuth centres in silica fbres containing no other dopants," Quantum Electron. **40**(7), 639–641 (2010).
7. E. G. Firstova, I. A. Bufetov, V. F. Khopin, V. V. Vel'miskin, S. V. Firstov, G. A. Bufetova, K. N. Nishchev, A. N. Gur'yanov, and E. M. Dianov, "Luminescence properties of IR-emitting bismuth centres in -based glasses in the UV to near-IR spectral region," Quantum Electron. **45**(1), 59–65 (2015).
8. E. Dianov, M. Melkumov, A. V. Shubin, S. Firstov, V. Khopin, A. Guryanov, and I. Bufetov, "Bismuth-doped fibre amplifier for the range 1300-1340 nm," Quantum Electron. **39**(12), 1099–1101 (2009).
9. V. Mikhailov, M. A. Melkumov, D. Inniss, A. M. Khegai, K. E. Riumkin, S. V. Firstov, F. V. Afanasiev, M. F. Yan, Y. Sun, J. Luo, G. S. Puc, S. D. Shenk, R. S. Windeler, P. S. Westbrook, R. L. Lingle, E. M. Dianov, and D. J. DiGiovanni, "Simple Broadband Bismuth Doped Fiber Amplifier (BDFA) to Extend O-band Transmission Reach and Capacity," presented at the *2019 Optical Fiber Communications Conference and Exhibition (OFC)* (2019).
10. M. A. Melkumov, I. A. Bufetov, A. V. Shubin, S. V. Firstov, V. F. Khopin, A. N. Guryanov, and E. M. Dianov, "Laser diode pumped bismuth-doped optical fiber amplifier for 1430 nm band," Opt. Lett. **36**(13), 2408–2410 (2011).
11. N. Taengnoi, K. R. H. Bottrill, Y. Hong, N. Thipparapu, C. Lacava, J. K. Sahu, D. J. Richardson, and P. Petropoulos, "4-level Alternate-Mark-Inversion for Reach Extension in the O-band Spectral Region," J. Lightwave Technol. (Early Access), 1–7 (2021).
12. N. Taengnoi, K. R. H. Bottrill, N. K. Thipparapu, A. A. Umnikov, J. K. Sahu, P. Petropoulos, and D. J. Richardson, "WDM Transmission with In-Line Amplification at 1.3μm Using a Bi-Doped Fiber Amplifier," J. Lightwave Technol. **37**(8), 1826–1830 (2019).
13. Y. Hong, K. R. H. Bottrill, N. Taengnoi, N. K. Thipparapu, Y. Wang, A. A. Umnikov, J. K. Sahu, D. J. Richardson, and P. Petropoulos, "Experimental Demonstration of Dual O + C-band WDM Transmission over 50-km SSMF with Direct Detection," J. Lightwave Technol. **38**(8), 2278–2284 (2020).
14. Y. Hong, H. Sakr, N. Taengnoi, K. Bottrill, T. Bradley, J. Hayes, G. Jasion, H. Kim, N. K. Thipparapu, Y. Wang, A. A. Umnikov, J. Sahu, F. Poletti, P. Petropoulos, and D. Richardson, "Multi-Band Direct-Detection Transmission Over an Ultrawide Bandwidth Hollow-Core NANF," J. Lightwave Technol. **38**(10), 2849–2857 (2020).
15. D. M. Baney, P. Gallion, and R. S. Tucker, "Theory and Measurement Techniques for the Noise Figure of Optical Amplifiers," Opt. Fiber Technol. **6**(2), 122–154 (2000).
16. R. Hui and M. O'Sullivan, "Characterization of Optical Devices," in *Fiber optic measurement techniques*, 259–363 (Academic Press/Elsevier, 2009).
17. N. Taengnoi, K. R. H. Bottrill, Y. Hong, Y. Wang, N. K. Thipparapu, J. K. Sahu, P. Petropoulos, and D. J. Richardson, "Experimental Characterization of Bismuth-Doped Fibre Amplifier: Electrical NF, PDG, and XGM," presented in the *2020 Conference on Lasers and Electro-Optics (CLEO)* (2020).
18. N. Thipparapu, A. Umnikov, P. Barua, and J. K. Sahu, "Bi-doped fiber amplifier with a flat gain of 25 dB operating in the wavelength band 1320–1360 nm," Opt. Lett. **41**(7), 1518–1521 (2016).

Optics EXPRESS

19. Y. Wang, N. K. Thipparapu, D. J. Richardson, and J. K. Sahu, "Ultra-broadband Bismuth-Doped Fiber Amplifier Covering a 115-nm Bandwidth in the O and E Bands," J. Lightwave Technol. **39**(3), 795–800 (2021).
20. N. K. Thipparapu, Y. Wang, S. Wang, A. A. Umnikov, P. Barua, and J. K. Sahu, "Bi-doped fiber amplifiers and lasers [Invited]," Opt. Mater. Express **9**(6), 2446–2465 (2019).
21. M. N. Zervas and R. I. Laming, "Rayleigh Scattering Effect on the Gain Efficiency and Noise of Erbium-Doped Fiber Amplifiers," IEEE J. Quantum Electron. **31**(3), 468–471 (1995).
22. P. Urquhart and T. J. Whitley, "Long span fiber amplifiers," Appl. Opt. **29**(24), 3503–3509 (1990).
23. M. Movassaghi, M. K. Jackson, V. M. Smith, and W. J. Hallam, "Noise figure of erbium-doped fiber amplifiers in saturated operation," J. Lightwave Technol. **16**(5), 812–817 (1998).
24. G. P. Agrawal and N. A. Olsson, "Self-Phase Modulation and Spectral Broadening of Optical Pulses in Semiconductor Laser Amplifiers," IEEE J. Quantum Electron. **25**(11), 2297–2306 (1989).
25. S. Hwang and K. Cho, "Gain tilt control of L-band erbium-doped fiber amplifier by using a 1550-nm band light injection," IEEE Photonics Technol. Lett. **13**(10), 1070–1072 (2001).
26. K. Thyagarajan, "Erbium-Doped Fiber Amplifiers," in *Guided Wave Optical Components and Devices*, 119–129 (Academic Press, 2006).
27. C. R. Giles, E. Desurvire, and J. R. Simpson, "Transient gain and cross talk in erbium-doped fiber amplifiers," Opt. Lett. **14**(16), 880–882 (1989).
28. Z. Zhu, X. Li, and Y. Xi, "A Polarization Insensitive Semiconductor Optical Amplifier," IEEE Photonics Technol. Lett. **28**(17), 1831–1834 (2016).
29. T. Panayiotou, N. Antoniades, and G. Ellinas, "On the impact of polarization-dependent gain/loss for optical multicast sessions," Opt. Express **22**(24), 29827–29834 (2014).
30. R. Sabella and P. Lugli, *High Speed Optical Communications* (Springer, 2012).